Distributed Sensor Systems

Matthias Weiß

Fraunhofer Institut für Hochfrequenzphysik und Radartechnik
FHR Passive Sensoren und Klassifizierung
Fraunhoferstraße 20, 53343 Wachtberg, Germany

E-Mail: matthias.weiss@fhr.fraunhofer.de

Abstract

Nowadays many surveillance systems are composed of multiple sensors to improve information content obtained from targets. Depending on constellation of sensors and targets, the performance of detection, localization, recognition, and tracking is improved dramatically. In particular a sensor network with distributed transmit and receive nodes can increase the probability to survive if any individual sensor node fails and the vulnerability against any electronic or physical attack is reduced [1]. Networks of homogeneous sensors even possess new processing concepts like multiple-input multiple-output (MIMO) or compressive sensing for data fusion and parameter estimation are supported.

The objective of this lecture is to establish a fundamental understanding of multi sensor systems to stimulate new concepts, theories, and applications in this area, and to provide a background to the following lectures of this series.

1.0 INTRODUCTION

Networks with multiple sensors promise to enhance existing surveillance systems in many aspects, which makes them an active area of research for many researchers and practitioners. For instance,

[0]Weiß, M. (2013) Distributed Sensor Systems. In *Radar and SAR Systems for airborne and space-based surveillance and reconnaissance* (pp. 1-1 — 1-22). STO-LS-SET-191, Paper 1. Neuilly-sur-Seine, France: STO. Available from: http://www.cso.nato.int/abstracts.aps.

if many sensors are involved in a network the capability of this system to survive increases if any individual sensor fails. Furthermore networks composed of different types of sensors delivers distinguishable information from the same object, even with co-located sensors, which improves target detection, identification, and classification, but not necessarily the localization accuracy. Such heterogeneous sensor networks rely on centralized architectures where the data from all sensors are fused and the information is extracted, as depicted in Fig. 1. Such centralized architectures are facing prob-

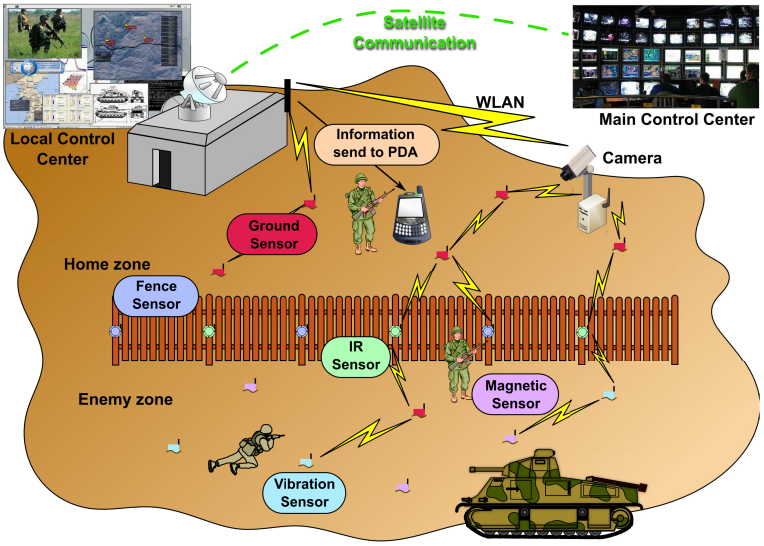

Fig. 1: A distributed heterogeneous sensor network.

lems with data rate via communication links and computational bottlenecks and are susceptible to total system failure if the central unit should fail.

In contrast to these networks with different types of sensors a network with homogeneous sensors enable a decentralised pre-processing with a central fusion stage. Designing a distributed network with only one type of sensor, for instance radar or sonar systems, enables new paradigms for constellations like bi-/multistatic, hitchhiker, or multiple-input multiple-output (MIMO) systems, and for signal processing. They provide higher resolution, better parameter identifiability due to joint estimation, which improves interference and jamming suppression, and fading mitigation. Likewise these networks possess a reduced vulnerability to electronic and physical attacks and can provide a counter stealth capability as targets will be seen from different aspect angles. Overall networks with homogeneous sensors where transmit and receive nodes are distributed over an area shows a significant improvement on target detection, parameter estimation and therefore also on tracking and recognition performance.

The sensor of choice for surveillance and reconnaissance systems is radar as its operation is not affected by any weather conditions (fog, rain, clouds, and sandstorm), is independent of time-of-day, and temperature, and can operate up to several thousands of kilometers. With this type of sensor a

continuous operation is realisable which is essential for military systems. Radar has gone through a technology evaluation over the years since his invention in 1904 by Christian Hülsmeyer [2], [3]. Progress in technology has opened new features in radar systems, like in the 1960s the phased-array antennas, allowing radars to change instantly search direction from pulse-to-pulse. Furthermore, computer performance has increased dramatically over time, which enables digital signal processing for radar applications, e.g. for adaptive array processing or space time adaptive processing (STAP). Over the past decades the progress in signal processing and wireless communication technology, where data throughput and link range was improved, allowed radar designers to consider distributed sensor networks based on Multi-Input Multi-Output (MIMO) techniques. [4]-[6]

Radar systems with distributed transmit and receive nodes illuminate the surveillance area simultaneously or in a time-multiplexed way with orthogonal waveforms from different locations and receive the reflected electromagnetic wave at spatially separated sites. due to this they shows significant potential for [7]-[11]:

- higher spatial and angle resolution,
- improved target detection, location, recognition, and tracking due to joint estimation,
- improved Doppler processing through diversity of look angles,
- mitigation of the problem of low radial velocities,
- interference and jamming suppression,
- fading mitigation,
- better handling of multiple targets,
- orthogonal waveforms increase information in the same bandwidth,
- higher sensitivity to detect slow moving targets,
- increased signal-to-noise ratio (SNR),
- increased electronic protective measures (EPM) capabilities.

Fig. 2 shows a distributed multiple-input multiple-output radar network. All nodes are transmitting orthogonal waveforms and receive the echoes simultaneously. All receivers perform a pre-processing and transmit their results to a central processing unit for data fusion and information extraction.

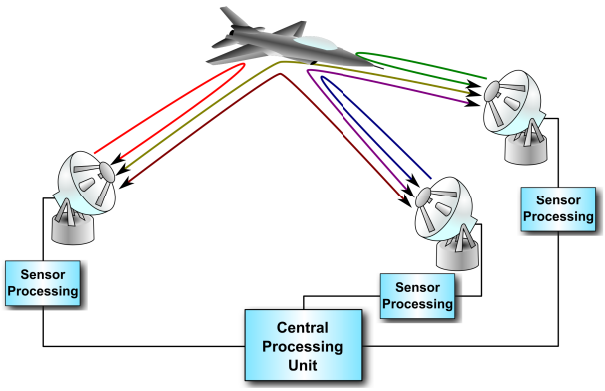

Fig. 2: A distributed multiple-input multiple-output radar network.

2.0 RADAR NETWORK

Besides the category of heterogeneous and homogeneous networks a further classification can be introduced to distinguish between them as:

- co-located sensor network and
- distributed sensor network.

Any combination of these first categories is practical, but in general different types of sensors are located nearby to ensure that the same area is observed. An example of a co-located homogeneous sensor network is a virtual linear array antenna, composed of several transmit and receive antennas grouped along a straight line [12]. For such configuration the signal processing has to be performed by a central processing unit, which ensures that the network operates coherently. A common architecture of distributed multi-sensor networks is to install a preprocessing at each receiver node and transfer the results over a high-speed communication link to a central processing stage for data fusion. Depending on the signal bandwidth, the complexity of the distributed network and on the communication link among the nodes and the central unit, also a central processing solution may be feasible [13].

The interests of system designers in distributed radar networks are seen in their enormous potential. Besides relatively simple designs, such as the case with a single illuminator and two receivers, extremely complex geometries can be constructed, with high demand on communication, processing and complex algorithms.

Examining the transmitter and receiver operation, a multistatic homogeneous network can be split into three principle categories of operation:

1. monostatic operation,
2. bistatic operation, and
3. any combination of the first two categories.

In the monostatic case, each node transmits a specific signal and receives and evaluates only the echo generated by his own signal. In a multistatic radar network a minimum of one illuminator and N spatially separated receivers observe a common area. In fact each transmit-receive pair is a bistatic radar. In the general case each network node acts as a transmitter and as a receiver and represents a fully MIMO radar system. Here, the receiver accepts echoes from all reflected signals. A schematic illustration of these different topologies is shown in Fig. 3.

A further categorisation is applicable, particularly if a node in the multistatic network is *active*, which means it is transmitting a dedicated signal, or *passive*. In the passive mode the receiver exploits illuminators of opportunity such as TV or radio broadcasts. Combining active and passive modes enhances covert operation of the multistatic network. For locating jammer sources passive operation in a network can be very useful. Jammers can be located with a multistatic radar network, based on

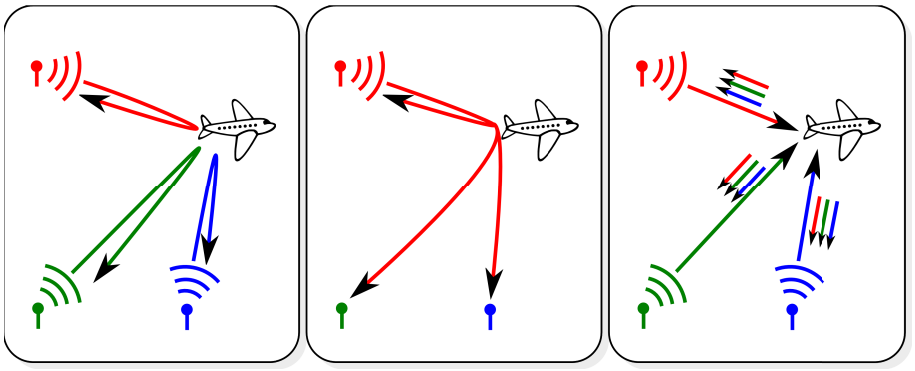

Fig. 3: Modes of operation: the multiple monostatic case, the multiple bistatic case and the fully multistatic case. The colored lines show the different waveforms used in each of the cases.

advanced cross correlation signal processing techniques, to provide their location through the time difference of the received jammer waveform at each receiver [14].

A fundamental problem with a distributed sensor network is linked to the established processing scheme, coherent and non-coherent signal processing. Compared to non-coherent systems the processing and information extraction from coherent networks is enhanced significantly. Especially in distributed networks spatial coherence has to be considered beside the temporal coherence. Spatial coherence is defined as the ability to maintain phase stability of the RF signals and interference among separated nodes [15]. Accordingly, sensor systems can likewise be grouped into the following three categories:

1. coherent networks,
2. short term coherent networks, and
3. incoherent networks.

In the first category each transmitter-receiver pair knows accurately the introduced phase-shift and can maintain it for a long period of time, for instance to determine the Doppler shift induced by the moving target or to perform signal processing in a synthetic aperture formation. To obtain increased target information from the scattered electromagnetic field (phase and amplitude) more complicated and demanding system concepts are required.

In a multistatic radar network of the second category, phase stability can only be maintained for a relatively short period. It permits joint signal processing so all information contained in the reflected signal can be extracted. This allows to plot and track using different receivers. The target position cannot be determined by phase, as achieved by the first network type, but it can be estimated through Time Difference of Arrival (TDOA) [16].

In an incoherent network a lot of power and available information from the target signal is unusable. The reason is that only the signal envelope can be used for extracting information while the phase

information is useless. This is harmful for specific signal processing tasks, for instance joint coherent signal processing for main lobe jamming cancelation.

In comparison among these categories, incoherent networks are the simplest to fabricate but have the disadvantages of the lowest sensitivity, least flexibility and highest information loss. Complexity and cost rise with the demand on coherence in the multistatic network.

3.0 GEOMETRY

Many of the particular problems of distributed radar networks result from various bistatic geometries with detached transmitter and receiver. A detailed analysis of the bistatic geometry was carried out by Jackson [17].

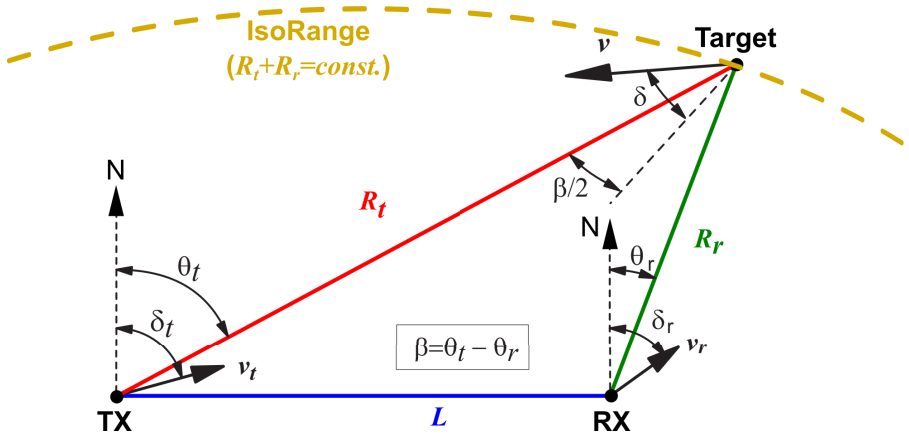

Fig. 4: North referenced bistatic geometry and notification. Also a contour of an iso-range line is shown.

In a bistatic configuration the transmit (TX) and receive (RX) node are separated by a distance called the baseline (denoted by L). A multistatic radar network can be considered as a composition of N different bistatic TX-RX pairs. In which each transmitter-receiver pair and target defines a bistatic plane. Hence, each new target defines a new bistatic plane. A monostatic radar is nothing but a bistatic pair with a baseline of length 0.

The target range for a monostatic radar is determined directly from the measurement of the signal travelling time τ from the transmitter to the target and back to the receiver. In the bistatic case the signal path is the sum $R = R_t + R_r$. R_t and R_r are now the ranges from target to TX and RX, respectively. In general $R_t \neq R_r$. To estimate R from τ the receiver must know the exact transmission time t_0, which means that the Tx-Rx pair must be synchronized in time. Furthermore, the receiver must know the transmitter location with respect to his own.

A characteristic measure that describes a bistatic geometry is the bistatic angle β, which is the angle between the two vectors from the target to TX and RX. It defines the position of the target on the iso-range contour, as described in Fig. 4. The iso-range contours are for far away targets ellipses with transmitter and receivers at the foci points. These contours changes to the well-known ovals of Cassini for targets nearby ($(R_t + R_r) < L$).

3.1 Bi-/Multistatic Radar Equation

The radar equation for a multistatic system is derived in a similar way to that for a monostatic radar. By the nature of a multistatic radar system, the potential SNR gains from all involved transmit/receive-pairs by MN, where N is the number of transmitters and M is the number of receivers. In the simplest form this is for a non coherent system:

$$SNR = \sum_{i=1}^{N} \sum_{n=1}^{M} \frac{P_t\, G_t(i)\, G_r(n) \sigma_b\, \lambda^2}{(4\pi)^3\, k\, T_0\, b\, F\, R_t^2(i) R_r^2(n)\, L_t} \tag{1}$$

where P_t is the transmit power, λ is the radar wavelength, $G_t(i)$ is the gain of the transmit antenna i, $G_r(n)$ is the gain of the receive antenna n, σ_b is the bistatic radar cross-section of the target, F is the receiver noise figure, R_t is the transmitter-to-target range, R_r is the target-to-receiver range, k is the Boltzmann's constant, T_0 is 290 K, b is the signal bandwidth, and L_t is the transmission loss. Each transmit-receive pair contributes to the overall system SNR, resulting in the MN gain if all sensors are synchronized and coherent signal processing takes place. In the non-coherent case the gain of the multistatic radar network is only N.

Contours of constant SNR are loci corresponding to $R_t(i)\, R_r(n) = \text{const.}$, which follow the lines of *ovals of Cassini* [17]. For monostatic radars the contours of constant signal-to-noise ratio are just circles for the 2-dimensional case or spheres centered on the radar in general.

3.2 Bistatic Range Resolution

The monostatic range resolution is defined by:

$$\Delta R_{mono} = \frac{\tau_p\, c_0}{2} = \frac{c_0}{2\, b} \quad , \tag{2}$$

with c_0 the speed of propagation, τ_p the (compressed) pulse width, and b the bandwidth of the transmitted signal.

This changes for a bistatic constellation as the contours of constant range are ellipse ($R = R_t + R_r = cont.$), with transmitter and receiver as the two foci points, as Fig. 5 shows. In order to separate two targets lying on different isorange contours they must be apart by [18]:

$$\Delta R_{bistatic} = \frac{\Delta R_{mono}}{\cos(\beta/2)} \tag{3}$$

For targets located on the transmitter-receiver baseline L the bistatic angle is $\beta = 180^\circ$ and, hence, can not be resolved as the range resolution is infinity.

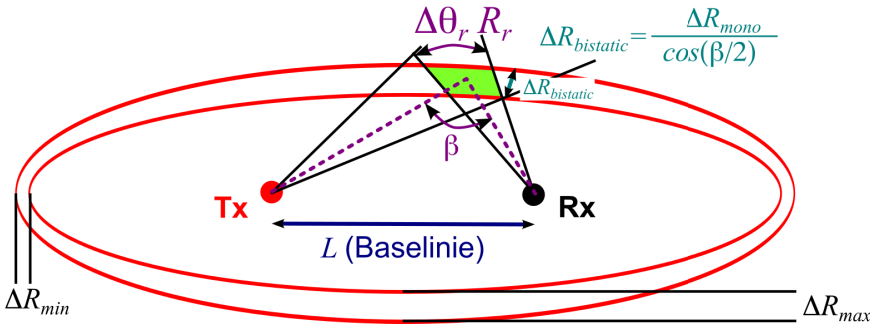

Fig. 5: Bistatic radar range resolution geometry.

3.3 Bistatic Clutter Cell Area

Clutter is part of the ground environment and effects the performance of any sensor system. In radar systems scattered energy from terrain interferes with the target signal. The interference depends on the bistatic angle β and is very important for the case of surface, volume clutters or non point scatterers and can be orders of magnitude larger than the echo from man-made targets as aircrafts or vehicles, as it is the case in bistatic applications like air, space, and ground surveillance of moving targets.

There is a distinction between the beam width and the range limited clutter cell area [17], [19]. The former depends on the transmit and receive antenna beam width at distance R_t and R_r, respectively and is expressed by:

$$A_{CB} = \frac{R_t \, \Delta\theta_t \cdot R_r \, \Delta\theta_r}{\sin \beta} \quad . \tag{4}$$

In Fig. 6 this area is highlighted in yellow.

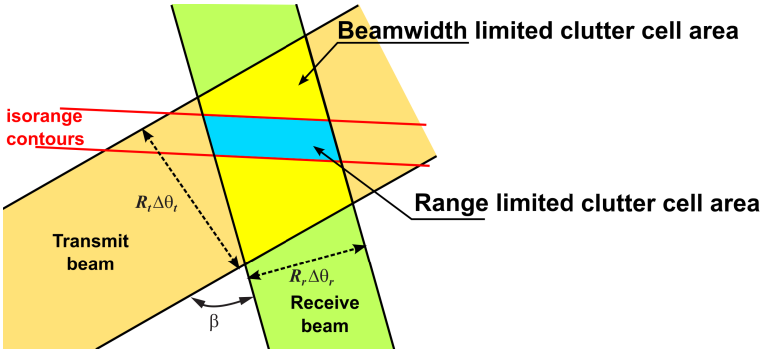

Fig. 6: Bistatic clutter cell

The range limited clutter cell area for small gazing angles and at large distance ($R_t + R_r \gg L$) is a parallelogram as shown in Fig. 6 by the blue highlighted region, with an area of:

$$A_{CR} = \frac{c \, \tau_p \, R_r \, \Delta\theta_r}{2 \cos^2(\beta/2)} \quad , \tag{5}$$

where τ_p is the compressed pulse width. It was assumed that the isorange contours are straight lines within the bistatic footprint. Furthermore the cross section of the transmit beam $R_t\,\Delta\theta_t$ is greater than that of the receiver beam $R_r\,\Delta\theta_r$, so the clutter area is determined only by the receiver characteristic.

In addition to the reflectivity of clutter/target depends on β it is always a game of numbers, where the clutter power is maximum and where it is minimum.

3.4 Bistatic Angular Resolution

A monostatic radar is able to distinguish two point targets located at the same distance R_m if they are apart more than 1.6 times the $3\,dB$ antenna beam width ($\Delta\theta_m \simeq \lambda/D_{Antenna}$) at their location. At a range of R this corresponds to a physical target separation of $\Delta_m = 1.6\,R\,\Delta\theta_m$. For bistatic radars generally $R_t\,\Delta\theta_t > R_r\,\Delta\theta_r$. Due to this assumption the transmitter beam is not contributing to the angular resolution. Therefore a bistatic radar can distinguish two targets located on the same isorange contour, as depicted in Fig. 7, if they are physically separated by Δ_B, where [20]:

$$\Delta_B \approx 1.6\,\frac{R_r\,\Delta\theta_r}{\sin\left((\pi-\beta)/2\right)} = 1.6\,\frac{R_r\,\Delta\theta_r}{\cos(\beta/2)} \tag{6}$$

The factor 1.6 ensures that the sum of both reflected signals has a drop of $0.6\,dB$ between the two maxima. Point targets separated only by a factor of 1 will cause in the processing scheme only a single maxima and, hence, can not be resolved. Usually, and specifically in passive coherent location, the cross-range dimension of the $3\,dB$ transmitter beam is larger than the receivers beam cross-range dimensions. Thus, it is too large to contribute to angular resolution and the receiving beam is playing the main role in the angular resolution.

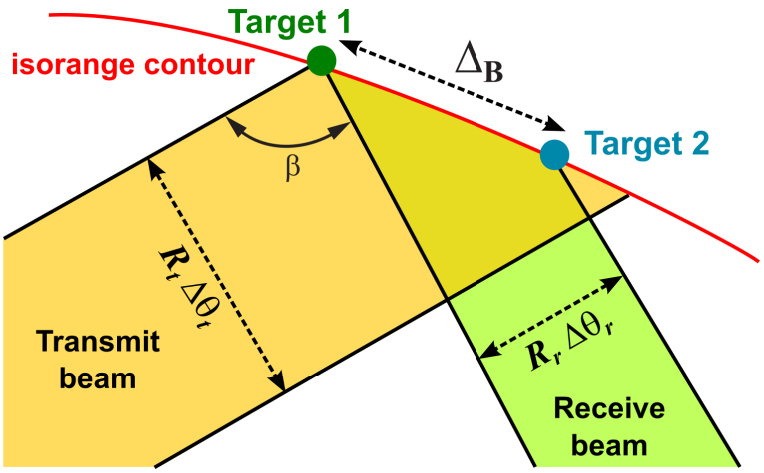

Fig. 7: Geometry for bistatic angular resolution.

3.5 Bistatic Doppler

The simple relation between motion of target and Doppler shift for a monostatic radar is no longer valid for bistatic constellations where the transmitter and receiver might exhibit different movements, as shown in Fig. 4. In general the equation can be quite complicated, as the time rate of change of the total path length from transmitter-target-receiver has to be taken into account [15]:

$$f_D = \frac{1}{\lambda}\left[\frac{\partial}{\partial t}\left(R_t + R_r\right)\right] = \frac{1}{\lambda}\left[\frac{\partial R_t}{\partial t} + \frac{\partial R_r}{\partial t}\right] \tag{7}$$

In the simplest case when only the target is moving the Doppler shift f_D can be determined by:

$$f_D = \frac{2\,v}{\lambda}\cos(\delta)\,\cos(\beta/2) \tag{8}$$

where v is the velocity of the target, λ is the radar wavelength, δ is the angle of the target velocity with respect to the bisector of the transmitter-target-receiver angle, and β is the bistatic angle. Some special cases of Eqn. (8) are shown in Tab. 1. Targets moving along the iso-range lines show zero Doppler and a maximum Doppler will occur if they are moving orthogonal to the constant bistatic range lines, which are ellipses for far away objects [17].

Tab. 1: Geometry dependent forms for Doppler shift of Eqn. (8)

β	δ	f_D	condition (geometry)
$0°$	$0°$	$(2v/\lambda)$	monostatic
$0°$	–	$(2v/\lambda)\cos(\delta)$	monostatic
$180°$	–	0	forward scatter
–	$\pm 90°$	0	$v \perp$ bisector
–	$\pm\beta/2$	$(2v/\lambda)\cos^2(\beta/2)$	$v \,\|\|$ TX or RX
–	$0°, 180°$	$\pm(2v/\lambda)\cos(\beta/2)$	$v \,\|\|$ bisector
–	$90° \pm \beta/2$	$\mp(2v/\lambda)\sin(\beta)$	$v \perp$ TX or RX LOS

In a radar network with distributed transmit and receive nodes a moving target will not exhibit zero Doppler shift to all receiving sites simultaneously. For this reason radar networks outperforms monostatic radar easily.

4.0 GETTINGDEEPER KNOLEDGEOF THE NETWORK

4.1 Ambiguity Function

An important tool to evaluate radar signal characteristics performance in terms of range and Doppler resolution as well as clutter rejection is the ambiguity function. The concept of the ambiguity function

was first introduced by *Woodward* [21]. It is a two dimensional function of time delay and Doppler frequency $\chi(\tau, f_D)$ showing the absolute envelope of the output of the receiver matched filter when the input to the filter is a Doppler shifted version of the original transmitted signal. The ambiguity function is determined only by the properties of the received pulse and the matched filter, which represents the transmitted pulse, and not any specific target scenario. There exists many definitions of the ambiguity function. Several of them focus on narrowband signals and others are applicable to describe the propagation delay and Doppler relationship of wideband signals [22]. For a complex baseband signal $s(t)$, which fulfils the narrowband condition $2vbT/c \ll 1$, with v the target velocity, b the signal bandwidth, T the pulse duration, and c the speed of propagation, the narrowband ambiguity function is given by [21]:

$$\left|\chi(\tau, f_D)\right| \quad = \quad \left| \int_{-\infty}^{\infty} s(t) \cdot s^*(t-\tau) \cdot e^{j2\pi f_D t}\, dt \right| \tag{9}$$

where * denotes the complex conjugate and f_D the Doppler shift in frequency. An important assumption for the target is that its scattering properties do not change over the pulse duration and with the look angles and that it is only slowly manoeuvring.

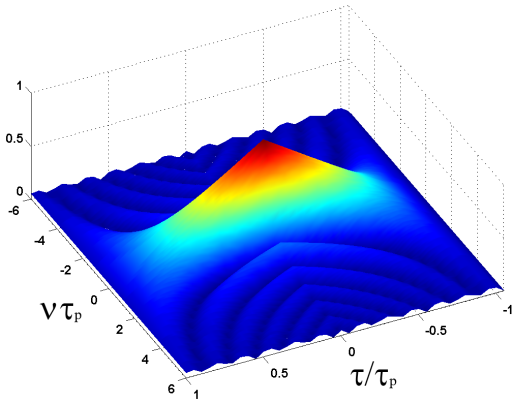

Fig. 8: Ambiguity function for a single rectangular pulse (pulse width t_p).

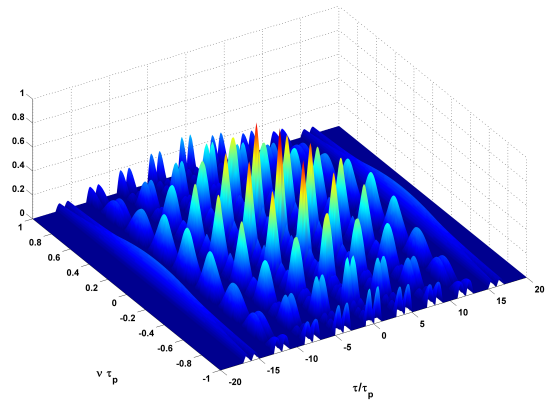

Fig. 9: Ambiguity function of a train of 5 rectangular pulses.

The monostatic ambiguity function was developed for a single co-located transmit/receive pair and is fairly well developed and understood [23]. It has been shown that the ambiguity function arises from the detection and parameter estimation problems joined with a slowly fluctuating point target being observed in additive white Gaussian noise. Fig. 8 shows the ambiguity function of a rectangular pulse with a duration of τ_p of a monostatic radar. If the signal processing takes 5 pulses into account the ambiguity function changes dramatically, as shown in Fig. 9.

For a bistatic geometry, the simple relationship between time delay τ and range r and target velocity v and Doppler shift f_D is no longer valid. Accordingly Tsao et al. [24] the bistatic ambiguity function

is:

$$\left|\chi\left(R_{R_H}, R_{R_A}, v_H, v_A, \theta_R, L\right)\right| = \left| \int s(t-\tau_A(R_{R_A}, \theta_R, L))\, s^*(t-\tau_H(R_{R_H}, \theta_R, L)) \cdot e^{-j2\pi(f_{D_H}(R_{R_H}, \theta_R, L) - f_{D_A}(R_{R_A}, \theta_R, L))\, t}\, dt \right| \quad (10)$$

where R_R and R_T are the ranges from the target to the receiver respectively to the transmitter, V is the target radial velocity, θ_R is the angle of the target measured from the receiver, L is the bistatic baseline, τ is the transmitter-target-receiver delay time, and the subscript H and A denote the hypothesized and actual values.

The important difference between the monostatic (9) and bistatic ambiguity function (10) is that the geometrical layout of the transmitter, receiver and target are now taken into account. This has a significant effect on the form of the ambiguity function and the resulting range and Doppler resolutions.

For a distributed radar network, which is nothing more than a composition of several transmit-receive-pairs, the ambiguity function is formulated based on the bistatic ambiguity function. It is assumed that the network is composed of M transmitters and N receivers. In that case the network shows MN bistatic pairs. To simplify the derivation of the multistatic ambiguity function the same assumptions are made as for the bistatic ambiguity function. Furthermore, it is assumed that the network is coherent. This implies that the echoes arriving at different time instances can be processed jointly. Similar to the bistatic radar ambiguity analysis, the multistatic radar ambiguity function is developed by the following three steps [13], [25]-[26]:

(i) For each transmitter-receiver-pair the bistatic ambiguity (10) function is calculated
(ii) Calculating a weighting factor according to received signal intensity

$$P_{ij} = \frac{P_i\, G_i\, G_j\, \lambda^2 \sigma_B}{(4\pi)^3\, R^2_{tx_i \to t}\, R^2_{t \to rx_j}} \quad (11)$$

$$w_{ij} = \frac{P_{ij}}{Max(P_{ij})} \quad (12)$$

(iii) To formulate multistatic radar ambiguity function using the results from previous calculations:

$$\chi_{multi} = \left| \frac{1}{M^2\, N^2} \sum_{i=1}^{M} \sum_{j=1}^{N} w_{ij} \chi_{ij} \right|^2 \quad (13)$$

In a bi-/multistatic radar system with separated transmitters and receivers the ambiguity function depends strongly on the constellation of nodes and target. For any further investigation the result should be split into different plots. The first diagram shows the result of the location accuracy in the x/y-plane where the second plot represents the solution for velocity and direction accuracy in a polar plot.

For a multistatic radar network consisting of 1 transmitter and 8 receivers, as depicted in Fig. 10, the ambiguity function was determined. The location of the transmit node is $x = 0\,\text{km}$ and $y = -6\,\text{km}$, which is identical with one receiver. The parameter of the simulation were $t_{pulse} = 40\,\mu\text{s}$, $PRF = 100\,\text{kHz}$, integration over 3 pulses, $f_c = 10\,\text{GHz}$, $v_{target} = 20\,\text{m/s}$.

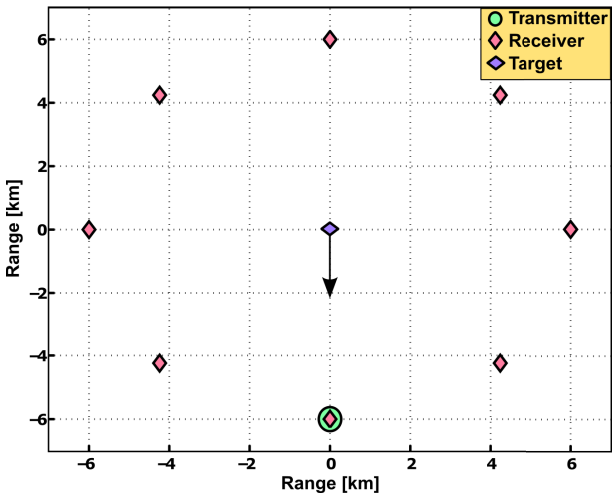

Fig. 10: Multistatic radar network consisting of one transmitter located at $x = 0\,\text{km}$ and $y = -6\,\text{km}$ and eight receivers. The moving target is located in the center.

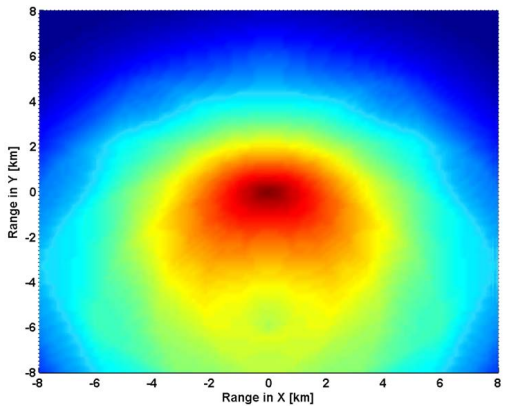

Fig. 11: Range plot of a multistatic ambiguity function.

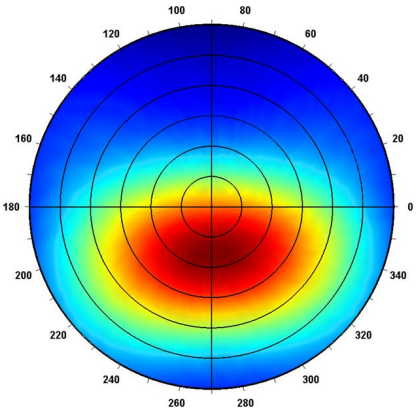

Fig. 12: Speed plot for a multistatic ambiguity function. Each circle represents an increase of $v = 10\,\text{m/s}$.

Fig. 11 shows the range plot of the multistatic ambiguity function. Clearly viable is the high localisation accuracy due to the distributed network. The polar plot in Fig. 12 shows that this constellation is able to determine the speed and direction of the target with high precision. Hence, evaluating the mulitstatic ambiguity function is a very useful tool to understand the achievable performance of a given distributed radar network taking the transmitted waveforms into account.

4.2 Target Localisation Accuracy

As already shown distributed sensor networks provide an improved target parameter estimation capability which makes them very attractive for system designers. In particular their increase of information content from each resolution cell, their improved angular resolution capability, and their ability to separate multiple targets [27], [28] their improved parameter identification [29], and their increased radar performance by exploiting radar cross section (RCS) diversity are very attractive for surveillance applications [30]. Likewise distributed radar networks can handle slow moving targets by exploiting Doppler estimates from multiple directions [31] and feature a highly accurate estimation of target position [32], [33].

An important aspect is the achievable localization accuracy of objects for a given constellation of transmitters and receivers in addition to system parameters such as signal bandwidth and antenna beam. For the following we assume a given radar network consists of M transmit and N receive nodes, which are located in the two-dimensional plane (x, y). The transmitters are located at $T_k = (x_{tk}, y_{tk})$, with $k = 1, ..., M$, and the coordinates of the receivers are $R_l = (x_{rl}, y_{rl})$. All transmitted signals are narrowband signals fulfilling the assumption of $(b/f_c)^2 \ll 1$. The target at the position $X = (x, y)$ has a complex radar cross section ζ, which is stable over the aspect angle, and, hence, the reflected signal from these targets possess a time delay τ_{lk}. With these assumptions the equivalent lowpass received signal at receiver l can be described by:

$$r_l(t) \;=\; \sum_{k=1}^{M} \zeta s_k(t - \tau_{lk}) e^{-j2\pi f_c \tau_{lk}} \;+\; n_l(t) \quad , \tag{14}$$

where $n_l(t)$ is the complex Gaussian white noise. The target location in the x/y-plane can be determined by the using the well-established multilateration principle, taking into account received signals from three or more receivers to resolve any ambiguities. In Eq. (14) the time delays τ_{lk} , which are determined by the location of the target, the transmitters, and receivers, are given by the following relation:

$$r_{lk} = D_l + D_k \;=\; \sqrt{(x_t - x)^2 + (y_t - y)^2} + \sqrt{(x_r - x)^2 + (y_r - y)^2} \tag{15}$$

To determine the position accuracy for a given constellation we assume that the range measurement in Eq. 15 has small errors. The linearising with a Taylor expansion around the target position $[x, y]^T$ yields:

$$r_{lk} \;+\; \delta_{lk} = D_1 + D_2 \;=\; \sqrt{(x_t - x)^2 + (y_t - y)^2} + \sqrt{(x_r - x)^2 + (y_r - y)^2} \tag{16}$$

$$\;=\; R_{lk}(x, y)\Big|_{@target} \;+$$

$$\frac{\delta\, R_{lk}(x, y)}{\delta x}\Big|_{@target} \cdot (x - x_t) \;+\; \frac{\delta\, R_{lk}(x, y)}{\delta y}\Big|_{@target} \cdot (y - y_t) \tag{17}$$

The position error can be rewritten in a matrix form [34]:

$$\delta_{lk} = \left[\frac{\delta R_{lk}(x,y)}{\delta x}\Big|_{@target} \quad \frac{\delta R_{lk}(x,y)}{\delta y}\Big|_{@target} \right] \cdot \begin{bmatrix} \delta_x \\ \delta_y \end{bmatrix} \tag{18}$$

with

$$\boldsymbol{\delta_{lk}} = \begin{bmatrix} \delta_{px} \\ \delta_{py} \end{bmatrix} \qquad \boldsymbol{\delta_x} = \begin{bmatrix} \delta_x \\ \delta_y \end{bmatrix} \tag{19}$$

Both error vectors are linked together via the transfer matrix $\boldsymbol{H}$

$$\boldsymbol{\delta_{lk}} = \boldsymbol{H}\boldsymbol{\delta_x} \quad \Rightarrow \quad \boldsymbol{\delta_x} = \boldsymbol{H}^{-1}\boldsymbol{\delta_{lk}} \tag{20}$$

The covariance matrix of a position error is defined by:

$$\boldsymbol{C}(\boldsymbol{\delta_x}) = E\left\{\boldsymbol{\delta_x}\boldsymbol{\delta_x}^T\right\} = E\left\{\boldsymbol{H}^{-1}\boldsymbol{\delta_{lk}}\boldsymbol{\delta_{lk}}^T\boldsymbol{H}^{T(-1)}\right\} = \boldsymbol{H}^{-1}\boldsymbol{C}(\delta_{lk})\boldsymbol{H}^{T(-1)} = (\boldsymbol{H}^T\boldsymbol{H})^{-1}\sigma^2_{UERE} \tag{21}$$

where σ_{UERE} is the standard deviation from the **u**ser **e**quivalent **r**ange **e**rror, which incorporates range resolution, receiver noise, and timing error all expressed in units of distance. Assuming that the measurement errors are independent and have similar average accuracy:

$$\boldsymbol{C}(\boldsymbol{\delta_{lk}}) = \begin{bmatrix} \sigma^2_{p1} & 0 \\ 0 & \sigma_{p2} \end{bmatrix} = \begin{bmatrix} \sigma^2_{UERE} & 0 \\ 0 & \sigma^2_{UERE} \end{bmatrix} = \boldsymbol{I}_{2x2}\,\sigma^2_{UERE} \tag{22}$$

The components of the matrix $(\boldsymbol{H}^T\boldsymbol{H})^{-1}$ quantify how range errors translate into components of the covariance of δx.

A valuable tool for visualizing location accuracy which can be achieved by a distributed sensor network is the Position Dilution of Precision (PDOP) mapping, which was originated with launching the Loran-C navigation system and came into much wider usage with GPS [35]-[38]. The dilution of precision can be interpreted as an expression which describes the impact of the positions of the transmit and receive nodes of a sensor network on the relationship between the estimated time delay and the localization errors. Hence, plots of PDOP give a deep insight into the achievable localization accuracy for a given distributed sensor network.

For each measurement error a corresponding dilution of precision can be defined. For the two dimensional case, where $X = (x, y)$, the horizontal dilution of precision (HDOP) is:

$$HDOP = \sqrt{\frac{\sigma_x^2 + \sigma_y^2}{\sigma^2_{UERE}}} \tag{23}$$

where σ_x^2 and σ_y^2 are the variances of the localization on the x and y axis, respectively. A relationship for HDOP is obtained in terms of the components of $(\boldsymbol{H}^T\boldsymbol{H})^{-1}$ by expressing $(\boldsymbol{H}^T\boldsymbol{H})^{-1}$ in component form

$$HDOP = \sqrt{\frac{\sigma_x^2 + \sigma_y^2}{\sigma^2_{UERE}}} = \sqrt{\frac{Tr\{\boldsymbol{C}\}}{\sigma^2_{UERE}}} = \sqrt{Tr\left\{\left(\boldsymbol{H}^T\boldsymbol{H}\right)^{-1}\right\}} \tag{24}$$

In Fig. 13 contour maps of the HDOP for two different radar networks are shown. Both radar networks consists of 4 transmitters and 4 receivers. In the left figure the nodes are equally placed on a circle. In the second case (right figure) the nodes are distributed on a semicircle. The green and red marks in

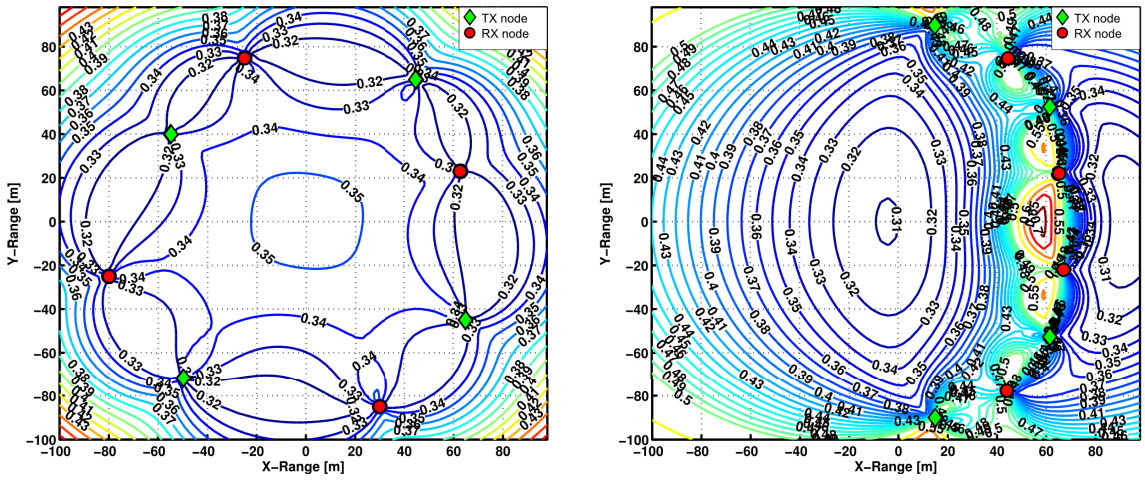

Fig. 13: HDOP contour plot with 4 transmit and 4 receive nodes in a network symmetrical placed. Left figure shows the achievable accuracy when the nodes are distributed among a circle and the right figure when nodes are located on a semicircle, respectively.

the HDOP plots represent the transmit and receive nodes of the radar network. Both plots show that the localization accuracy is very high (low PDOP values) if targets are located inside a sensor network compared to targets located outside of the *system*. Hence, locations of transmitters and receivers has to be chosen carefully to obtain the demanded accuracy.

Maps of PDOP represent a very useful tool for showing the accuracy which can be obtained for a given sensor node constellation or for choosing the best node locations to cover a given surveillance area.

5.0 PROBLEMS ASSOCIATED WITH SENSOR NETWORKS

An essential issue in designing a sensor network is synchronisation among all nodes. For a coherent system information extraction and processing is more efficient compared to non-coherent networks. Besides temporal coherence in time, frequency, and phase, the spatial coherence has to be considered in a distributed sensor system. The spatial coherence is defined as the ability to maintain phase stability of the RF signals and interference between separated stations [15].

5.1 Time Synchronisation

For range measurements synchronisation in time is needed between transmit and receive nodes and typically an accuracy in the order of a fraction of the transmitted pulse τ_p is required. For a compressible pulse, where more than one sinusoidal wave is transmitted, this is equal to $\tau_p = 1/b$, with b the signal bandwidth [15].

If the network nodes are not too far separated from each other synchronising the stable local oscillators can be achieved by connecting them together by cable, fibre or direct communication link. If no direct line of sight is available, time synchronisation can also be achieved via a scattering signal from a persistent scatterer. A prerequisite is that the scattering volume is detected by transmit and receive antenna lobes. This method is not suitable to stabilize two local oscillators via a phase-locked loop as one can expect a large variation (jitter) in the time base if the scattering body moves, for instance by gusts of wind.

Commercially available are a range of various qualities of stable oscillators ranging from a simple quartz oscillators, temperature controlled quartz with single or double ovens for stable operating temperature, to more expensive atomic clocks such as rubidium or caesium oscillators, as shown in Tab. 2.

Tab. 2: Comparison of various stable oscillators at 10 MHz

	TCXO	OCXO	OCXO(BVA)	MCXO	Rubidium	Cesium	GPS
temperature stability	$1{\cdot}10^{-6}$	$2{\cdot}10^{-8}$	$1{\cdot}10^{-10}$	$2{\cdot}10^{-8}$	$2{\cdot}10^{-8}$	$2{\cdot}10^{-8}$	—
drift per day	$1{\cdot}10^{-8}$	$1{\cdot}10^{-10}$	$5{\cdot}10^{-12}$	$5{\cdot}10^{-11}$	$5{\cdot}10^{-13}$	$3{\cdot}10^{-14}$	$3{\cdot}10^{-14}$
short-time stability $\sigma_y(\tau)$	$1{\cdot}10^{-9}$	$1{\cdot}10^{-12}$	$5{\cdot}10^{-13}$	$1{\cdot}10^{-10}$	$5{\cdot}10^{-12}$	—	—
1s	$1{\cdot}10^{-10}$	$1{\cdot}10^{-11}$	$1{\cdot}10^{-12}$	$2{\cdot}10^{-8}$	$1{\cdot}10^{-11}$	$6{\cdot}10^{-11}$	—
100 s	$3{\cdot}10^{-10}$	$1{\cdot}10^{-11}$	$1{\cdot}10^{-12}$	$2{\cdot}10^{-8}$	$1{\cdot}10^{-13}$	$6{\cdot}10^{-12}$	—
1 day	$1{\cdot}10^{-12}$	$3{\cdot}10^{-12}$	$3{\cdot}10^{-12}$	$5{\cdot}10^{-10}$	$1{\cdot}10^{-13}$	$6{\cdot}10^{-12}$	—
$\mathcal{L}$ @ 1Hz	-50	-100	-122	-115	-80	-85	—
$\mathcal{L}$ @ 10Hz	-80	-130	-137	-135	-98	-125	—
$\mathcal{L}$ @ 100Hz	-110	-140	-145	-145	-137	-135	—
$\mathcal{L}$ @ 1kHz	-120	-145	-156	-150	-150	-140	—

Due to the inherent aging and instability, the local references must be continuously re-synchronised on a time interval, which depends on the required stability and coherence in the network. The stability directly influences the coherent integration time in the sensor network.

If no direct synchronisation is possible, as the baseline is too large for any cable or fibre, or no line-of-sight exists, the local oscillators of each network node can be indirectly synchronised by use of a Global Navigation Satellite System (GNSS) which provides a highly stable time reference. This time

reference, the 1 Pulse-Per-Second (PPS) signal, can be used to discipline the local oscillator [39]. The uncertainty in time of a 1PPS is in the order of 100 ns or less. If two GNSS receivers are receiving navigation signals from the same satellites, which is possible up to a distance of 8000 km between them, an accuracy of 5...20 ns can be achieved, even if the selective available (SA) signal is activated. Only the location of the GNSS receiver must be known precisely ($\leq$ 1 m). This can be easily obtained by an averaging of the calculated position from the GNSS data over several days. Figure 14 shows the phase difference between two temperature controlled crystal oscillators which were disciplined by different GPS receivers and their PPS signal. The standard deviation of the 1PPS signal was 50 ns for each GPS receiver. Each GPS receiver has been set into the mobile mode, which means that the receiver has to solve the full set of equations to determine the position and time for each GPS epoch. Therefore, a lower variance can be expected if both GPS units works in the *stationary mode*, where the location of the GPS receiver is known and only the time has to be determined from the GPS signals [39].

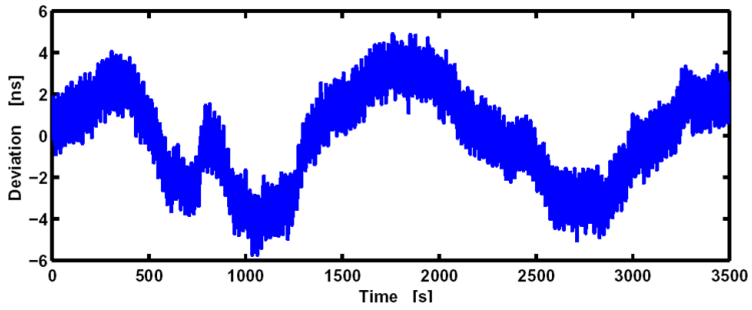

Fig. 14: Measured phase difference between two GPS disciplined TCXO units at 10 MHz.

In this configuration the local oscillator determines the short time stability, while the long time stability is determined by the stability of the GPS system. As long as the receiver is locked to the GPS, the long time stability is ensured. In the case of GPS jamming or receiver unlock, the stability of the local oscillator unit will determine the drift due to aging and temperature changes etc.

In general the required time stability depends on the local oscillators stability and on the update interval and can be determined by [15]:

$$Timestability \quad \leq \quad \frac{\Delta\tau_{required}}{T_{update\_intervall}} \quad . \tag{25}$$

If the synchronisation of the local oscillators takes place by disciplining them to an additional time reference, as it is the case of locking the local clocks to the GPS time source, the time stability has to be an order of 2 higher.

Another important aspect in selecting local oscillators for a distributed radar network is their phase noise characteristic. While in a single sensor system and its monostatic operation the received echo has some correlation with the transmitted signal, even at great distances, such a correlation does not

exist in a multistatic network with several independent reference clocks. Particularly for detecting slow moving targets which introduce a small Doppler shift a low phase noise close to the carrier is very important for the Doppler processing.

5.2 Phase Synchronisation

For Doppler or moving target indication (MTI) processing there must exist phase coherence between transmit and receive nodes, which enables the rejection of clutter or chaff. Phase coherence can be obtained in the same ways as time coherence. Using indirect phase synchronisation, which is the best solution, involves high-precision oscillators at the network nodes that are re-synchronised via the 1PPS provided by GNSS receivers. Over the whole coherent integration time τ_k the phase stability has to be guaranteed and equal to $\Delta\phi \,/\, 2\pi f \tau_k$ [15]. For a ground based bistatic radar with a center frequency of 3 GHz, a maximum phase deviation of $\Delta\phi = 4^\circ = 0,07\,\mathrm{rad}$ and a coherent integration time of $\Delta\tau_k = 1\,\mathrm{ms}$ the required oscillators stability is $3.7 \cdot 10^{-12}$. This requirement can be fulfilled with a temperature-controlled crystal oscillator, as can be taken from Tab. 2.

If a line-of-sight exists phase synchronisation is obtainable by a direct signal. If the synchronisation takes place with each transmitted pulse a phase stability can be reached of $\Delta\phi \,/\, 2\pi f \Delta T_{rt}$, with ΔT_{rt} denoting the travelling time difference between transmitter-target-receiver and the direct signal. $\Delta\phi$ is the allowed phase difference in *rad*. If an accuracy of $\Delta\phi = 4^\circ = 0,07\,\mathrm{rad}$ is requested at a center frequency of $f = 10\,\mathrm{GHz}$ and the time difference $\Delta T_{rt} = 1\,\mathrm{ms}$ ($\Delta r_{rt} = 300\,\mathrm{km}$) the oscillator must have a stability of 10^{-9}, which can easily be achieved by a simple quartz oscillator.

6.0 CONCLUSION

This tutorial has attempted to provide an introduction to distributed sensor systems, in particular in radar. Current interest in multistatic radar networks are high as bistatic approaches provides solutions to several problems relating to monostatic systems. Due to technology progress over recent years in signal processing, synchronization, wireless communications, and navigation, practical systems are deployed and operated around the world.

7.0 REFERENCES

[1] D. W. O'HAGAN, M. UMMENHOFER, H. KUSCHEL, J. HECKENBACH, "A Passive/Active Dual Mode Radar Concept", 14th International Radar Symposium IRS 2013l, Dresden, pp.: 136–142

[2] C. HÜLSMEYER, "Patent DE165546: Verfahren, um metallische Gegenstände mittels elektrischer Wellen einem Beobachter zu melden.", 30. April 1904

[3] C. HÜLSMEYER, "Patent DE169154: Verfahren zur Bestimmung der Entfernung von metallischen Gegenständen (Schiffen o. dgl.), deren Gegenwart durch das Verfahren nach Patent 16556 festgestellt wird.", 11. Nov. 1904

[4] J.G. FOSCHINI, "Layered space-time architecture for wireless communication in a fading environment when using multiple antennas", Bell Labs Technical Journal, Vol. 1, pp. 41-59, 1996.

[5] N.B. SINHA, R. BERA, AND M. MITRA, "Digital array mimo radar and its performance analysis", Progress In Electromagnetics Research C, Vol. 4, pp. 25-41, 2008

[6] J.G. FOSCHINI AND M.J. GANS, "On the limits of wireless communications in a fading environment when using multiple antennas", Wireless Pers. Commun., Vol. 6, pp. 311-335, 1998.

[7] D.W. BLISS AND K.W. FORSYTHE, "Multiple-input multiple-output (MIMO) radar and imaging: Degrees of freedom and resolution", Conf. Record 37th Asilomar Conf. Signals, Systems & Computers, Pacific Grove, CA, Nov. 2003, Vol. 1, pp. 54-59.

[8] R.T. HOCTOR AND S.A. KASSAM, "The unifying role of the coarray in aperture synthesis of coherent and incoherent imaging", Proc. IEEE 78(4), pp. 735 -752 (April 1990)

[9] K.W. FORSYTHE, D.W. BLISS, AND G.S. FAWCETT, "Multiple-input multiple-output (MIMO) radar performance issues", Proc. 38th IEEE Asilomar Conf. Signals, Systems, and Computers, Nov. 2004, pp. 310-315.

[10] H. GRIFFITH, "Bistatic: introduction and historical background", NATO SET-136 Lecture Series, 2009

[11] J. LI AND P. STOICA, "MIMO radar signal processing", John Wiley & Sons, Inc., Hoboken, New Jersey, 2009

[12] M. WEISS, "Digital Antenna", NATO SET-136 Lecture Series "Multistatic Surveillance and Reconnaissance: Sensor, Signals and Data Fusion", April 2009

[13] C. BAKER, "Multistatic Radar Processing and systems", NATO SET-136 Lecture Series "Multistatic Surveillance and Reconnaissance: Sensor, Signals and Data Fusion", April 2009

[14] R.J.E. POLLARD; D.M. GOULD, "Bistatic Sensor Cross Correlation for Emitter Location", 28th European Microwave Conference, Oct. 1998, Vol. 1, pp.:540-545

[15] NICHOLAS J. WILLIS, "Bistatic Radar", Artech House, Boston, London, 1991

[16] JIŘÍ HOFMAN, JAN BAUER, "Tajemství radiotechnického pátrače Tamara [The Secret of Radiotechnical Sensor Tamara]", 2003, ISBN 80-86645-02-9

[17] M.C. JACKSON, "The geometry of bistatic radar systems," Communications, Radar and Signal Processing, IEE Proceedings Part F , vol. 133, no. 7, pp. 604-612, December 1986

[18] EDITED BY N.J. WILLIS AND H.D. GRIFFITHS, "Advances in Bistatic Radar", SciTech Publishing Inc., Raleigh, NC, ISBN 1891121480, 2007

[19] NICHOLAS J. WILLIS, ED. MERRILL SKOLNIK, "Bistatic Radar, Chapter in: Radar Handbook", 2.Ed, McGraw-Hill Inc., 1990

[20] MARINA GASHINOVA, LIAM DANIEL, EDWARD HOARE, VLADIMIR SIZOV, KALIN KABAKCHIEV, MIKHAIL CHERNIAKOV, "Signal characterisation and processing in the forward scatter mode of bistatic passive coherent location systems", EURASIP Journal on Advances in Signal Processing 2013, doi:10.1186/1687-6180-2013-36

[21] P.M. WOODWARD, "Probability and Information Theory with Applications to Radar", Pergamon, New York, 1953

[22] L. SIBUL, L. ZIOMEK, "Generalised wideband cross ambiguity function", IEEE International Conference on Acoustics, Speech, and Signal Processing, ICASSP '81.01/05/198105/1981; pp. 1239–1242

[23] N. LEVANON, "Radar principles", Wiley, 1998

[24] T. TSAO, M. SLAMANI, P. VARSHNEY, D. WEINER, H. SCHWARZLANDER, S. BOREK, "Ambiguity function for a bistatic radar", IEEE Transactions on Aerospace and Electronic Systems, Vol. 33, No. 3, July 1997, pp. 1041-1051

[25] G. SAN ANTONIO, D. FUHRMANN, F. ROBEY, "MIMO radar ambiguity functions," IEEE Journal of Selected Topics in Signal Processing, Vol. 1, No. 1 (2007)

[26] T. DERHAM, S. DOUGHTY, C. BAKER, K. WOODBRIDGE, "Ambiguity Functions for Spatially Coherent and Incoherent Multistatic Radar," IEEE Trans. Aerospace and Electronic Systems, Jan. 2010, pp. 230-245, DOI: 10.1109/TAES.2010.5417159

[27] F.C. ROBEY, S. COUTTS, D. WEIKLE, J.C. MCHARG, K. CUOMO, "MIMO radar theory and experimental results", in Proc. of 37th ASILOMAR 2004 Conf. on Signals, Systems and Computers, Nov. 2004, pp. 300-304

[28] I. BEKKERMAN, J. TABRIKIAN, "Target detection and localization using MIMO radars and sonars", IEEE Trans. on Sig. Proc., Vol. 54, Oct. 2006, pp. 3873-3883

[29] L. XU, J. LI, P. STOICA, "Adaptive techniques for MIMO radar" in 14th IEEE Workshop on Sensor Array and Multi-channel Processing, Waltham, MA, July 2006.

[30] E. FISHLER, A.M. HAIMOVICH, R.S. BLUM, L. CIMINI, D. CHIZHIK, R. VALENZUELA, "Spatial diversity in radars - models and detection performance", IEEE Trans. on Sig. Proc., Vol. 54, pp. 823-838, March 2006

[31] N. LEHMANN, A.M. HAIMOVICH, R.S. BLUM, L. CIMINI, "MIMO - radar application to moving target detection in homogenous clutter", 14th IEEE Workshop on Sensor Array and Multi-channel Processing, Waltham, MA, July 2006

[32] N. LEHMANN, A.M. HAIMOVICH, R.S. BLUM, L. CIMINI, "High resolution capabilities of MIMO radar", Proc. of 40th ASILOMAR 2006 Conference on Signals, Systems and Computers, Nov. 2006

[33] H. GODRICH, A.M. HAIMOVICH, R.S. BLUM, "Cramer Rao Bound on Target Localization Estimation in MIMO Radar Systems", in Proc. of CISS Conf., March 2008.

[34] ELLIOTT D. KAPLAN, CHRISTOPHER J. HEGARTY, "Understanding GPS -Principles and Applications-", Artech House, Boston, London, 2006

[35] R.B. LANGELEY, "Dilution of Precision", GPS World, May 1999, pp. 52-59

[36] H.B. LEE, "A novel procedure for assessing the accuracy of the hyperbolic multilateration systems", IEEE Trans. on Aerospace and Electronic Systems, Vol. 11, Jan. 1975, pp. 2-15

[37] N. LEVANON, "Lowest GDOP in 2-D scenarios", IEE Proc. Radar, Sonar, Navigation, Vol. 147, June 2000, pp. 149-155

[38] R. YARLAGADDA, I. ALI, N. AL-DHAHIR, J. HERSHEY, "GPS GDOP metric", IEE Proc. Radar, Sonar, Navigation, Vol. 147, No. 5, October 2000, pp. 259-264

[39] M. WEISS, "Synchronization of bistatic Radar systems", IEEE 2004 International Geoscience and Remote Sensing Symposium, Anchorage, Alaska, USA, pp. 1750-1753